

The Inhibition of Tin Whiskers on the Surface of Sn-8Zn-3Bi-0.5Ce Solders

C.C. Jain, C.L. Chen, H.J. Lai, and T.H. Chuang

(Submitted March 1, 2010)

Through the refinement of the (Ce, Zn)Sn₃ intermetallic phase, the formation of tin whiskers, previously observed on the surface of a Sn-3Ag-0.5Cu-0.5Ce solder, was prevented in a Sn-9Zn-0.5Ce alloy. However, whisker growth can still occur on the surface of Sn-8Zn-3Bi-0.5Ce solder after air storage at room temperature and at 150 °C due to the formation of large (Ce, Zn)Sn₃ intermetallic clusters. Further experiments showed that decreasing the Bi-content in this Sn-8Zn-0.5Ce alloy to 1 and 2 wt.% can recover the beneficial effects of Zn additions on the refinement of the (Ce, Zn)Sn₃ phase and obviously reduce the appearance of tin whiskers. In addition, alloying the Sn-8Zn-3Bi-0.5Ce solder with 0.5 wt.% Ge, which increases the oxidation resistance of the (Ce, Zn)Sn₃ intermetallic clusters, can also effectively inhibit tin whisker growth.

Keywords (Ce, Zn)Sn₃ intermetallics, rare earth, Sn-Zn-Bi-Ce-Ge, whisker

1. Introduction

Addition of rare earth (RE) elements in solder alloys has been reported to have improved effects on their physical and mechanical properties. Ma et al. (Ref 1) showed that the intermetallic compounds at the interface of Sn-40Pb solder joints doped with 0.05 wt.% La were inhibited, through which fatigue life increased by a factor of three. For the development of Pb-free solders, Wu et al. (Ref 2) found that a Sn-3.5Ag containing 0.25 wt.% mixed metal (Ce, La) revealed better wettability, tensile strength, and creep resistance than undoped Sn-3.5Ag alloy. Wu et al. further indicated that the grain size of a Sn-0.7Cu solder alloy with 0.5 wt.% mixed metal was refined, which led to a fine and uniform distribution of Cu₆Sn₅ intermetallic compounds in the solidified matrix. The modification of microstructure resulted in significant improvements of its strength and microhardness. In addition, the microstructure of such a Sn-0.7Cu-RE solder was more stable than that of the undoped Sn-0.7Cu alloy and had higher creep resistance (Ref 3). Chen et al. (Ref 4) added 0.2 wt.% mixed metal (Ce, La) into a Sn-3.8Ag-0.7Cu solder, with the result that the microstructure and Ag₃Sn precipitates were refined, which led to an increase of creep rupture life of seven folds. For the Sn-Ag-Cu solders, Dudek et al. (Ref 5) reported that the rupture strain of a Sn-3.9Ag-0.7Cu-0.5La increased nearly 150% over that of the undoped alloy. The beneficial effects of

RE addition have also been demonstrated in Sn-9Zn solder. Wu et al. (Ref 6) showed that Sn-9Zn-RE solder exhibited finer β-Sn grains and higher tensile strength than undoped Sn-9Zn alloy. In addition, the wettability of Sn-9Zn-RE solder was greatly improved due to the decrease of surface tension. Summarizing these experimental results, it is clear that RE elements will play an important role in developing high performance Pb-free solders.

However, Chuang and Yen (Ref 7) observed that long fiber- and hillock-shaped whiskers grew rapidly on the surface of a Sn-3Ag-0.5Cu-0.5Ce solder after air exposure at room temperature and 150 °C, respectively. It has been proposed that the mechanism for the rapid whisker growth in this Ce-doped solder is the predominate oxidation of RE containing CeSn₃ intermetallic phase existing in its alloy matrix, which leads to a compressive stress that extrudes the tin atoms out of the specimen surface (Ref 8). Since the occurrence of tin whiskers might result in the short circuits of devices and the failure of electronic products, the inhibition of whisker growth is an important task for the alloying design of Pb-free solders through the addition of RE elements. Fortunately, our recent study shows that such a phenomenon of rapid whisker growth in RE-containing solders is absent in a Sn-9Zn-0.5Ce alloy (Ref 9). Further study indicated that the elimination of tin whiskers can also be obtained in the Sn-3Ag-0.5Cu-0.5Ce solder through alloying with 0.5 wt.% Zn (Ref 10). The prevention of tin whiskers in both the cases has been suggested to be attributable to the small size of the (Ce, Zn)Sn₃ intermetallic phase in this alloy.

However, this article presents an interesting result, that fiber-shape whiskers can still be found on the surface of a Sn-8Zn-3Bi-0.5Ce solder air-stored at room temperature and at 150 °C due to the formation of large (Ce, Zn)Sn₃ clusters in this alloy. Further study shows that decreasing the Bi-content to 1 or 2 wt.% can prevent the whisker growth through the refining of (Ce, Zn)Sn₃ clusters. In addition, alloying with 0.5 wt.% Ge in the Sn-8Zn-3Bi-0.5Ce solder, which increases the oxidation resistance of its (Ce, Zn)Sn₃ intermetallic clusters, can also effectively alleviate the occurrence of tin whiskers.

C.C. Jain, C.L. Chen, and T.H. Chuang, Department of Materials Science and Engineering, National Taiwan University, Taipei 106, Taiwan; and H.J. Lai, Materials Research Laboratories, Industrial Technology Research Institute, Hsinchu 31015, Taiwan. Contact e-mail: tunghan@ntu.edu.tw.

2. Experimental

For the experiments, Sn-8Zn-3Bi, Sn-8Zn-3Bi-0.5Ce, Sn-8Zn-3Bi-0.5Ce, Sn-8Zn-2Bi-0.5Ce, and Sn-8Zn-1Bi-0.5Ce-0.5Ge were molten at 1000 °C in 10^{-5} Torr vacuum. The solidus and liquidus of these solder alloys were measured using a differential scanning calorimeter (DSC), and the results are listed in Table 1. The as-cast ingots were then cut with a diamond saw, and their cross sections were ground with 2000 grit SiC paper and polished with 0.3 μm Al_2O_3 powder. Some specimens were naturally exposed at room temperature in air, while others were stored at 150 °C in an air furnace. The microstructure of the alloys and the morphology of tin whiskers was observed with a scanning electron microscopy (SEM). The chemical compositions of the various phases appearing in the metallographic images were analyzed with energy dispersive x-ray spectrometry (EDX). For this purpose, at least five measurements were performed for each phase, and the average values are presented in Table 2 to 4 for the various Ce-doped alloys in this study.

3. Results and Discussion

Although the addition of RE elements has been reported to show the effect of melting point depression in solder alloys,

DSC analyses in this study indicated that both the solidus and the liquidus temperatures of the Sn-8Zn-3Bi alloy rose with the addition of 0.5 wt.% Ce (Table 1). Further doping with 0.5 wt.% Ge caused a higher solidus and liquidus as compared with the Sn-8Zn-3Bi and Sn-8Zn-3Bi-0.5Ce alloys. In addition, the solidus and liquidus of Sn-8Zn-3Bi-0.5Ce alloy were found to increase with the decrease of Bi content.

The microstructure of Sn-8Zn-3Bi solder contained thin plates of Zn-rich precipitates (black in color) and fine particles of Bi-rich phase (white in color) in the Sn-rich matrix, as shown in Fig. 1(a). The chemical compositions (at.%) of the solder matrix were Sn:Zn:Bi:O = 89.9:3.4:2.5:4.2. The active Zn element in this alloy caused the early oxidation of its solder matrix during preparation of the metallographic specimens.

Adding 0.5 wt.% Ce into this Sn-8Zn-3Bi alloy led to the appearance of many large cluster-shaped phases about 10 μm in size, as shown in Fig. 1(b). EDX analyses indicated that the Sn-rich solder matrix of this Sn-8Zn-3Bi-0.5Ce solder contained 2.2 at.% Bi, 13.5 at.% O and negligible Ce. The much higher oxygen content in this alloy, as compared to the Ce-free alloy, should be attributed to the very high chemical activity and oxidation tendency of Ce. In addition, Table 2 shows that the cluster-shaped phases possessed a composition (at.%) of Sn:Zn:Bi:Ce:O = 57.5:7.3:2.3:17.2:15.7, which corresponds to a (Ce, Zn)Sn₃ intermetallic phase. The appearance of such large intermetallic clusters in this Sn-8Zn-3Bi-0.5Ce alloy is in contrast to that observed previously in a Sn-9Zn-0.5Ce solder,

Table 1 Solidus and liquidus of Sn-8Zn solders doped with 3Bi, 2Bi, 1Bi, 0.5Ce, and 0.5Ge in this study

	Sn-8Zn-3Bi	Sn-8Zn-3Bi-0.5Ce	Sn-8Zn-2Bi-0.5Ce	Sn-8Zn-1Bi-0.5Ce	Sn-8Zn-3Bi-0.5Ce-0.5Ge
Solidus	195.40 °C	197.11 °C	198.11 °C	198.73 °C	197.79 °C
Liquidus	196.70 °C	199.03 °C	199.91 °C	200.51 °C	199.18 °C

Table 2 Chemical compositions of the various phases in the Sn-8Zn-3Bi-0.5Ce solder

	Sn, at.%	Zn, at.%	Bi, at.%	Ce, at.%	O, at.%
Solder matrix	80.4	3.7	2.2	0.3	13.4
(Ce, Zn)Sn ₃ before air storage	57.5	7.3	2.3	17.2	15.7
(Ce, Zn)Sn ₃ after air storage at RT	42.5	8.4	2.2	17.9	29.0
(Ce, Zn)Sn ₃ after air storage at 150 °C	37.4	7.9	2.5	18.4	33.8

Table 3 Chemical compositions of the various phases in the Sn-8Zn-2Bi-0.5Ce solder

	Sn, at.%	Zn, at.%	Bi, at.%	Ce, at.%	O, at.%
Solder matrix	81.9	3.6	1.5	0.4	12.6
(Ce, Zn)Sn ₃ before air storage	55.2	7.5	1.7	17.8	17.8
(Ce, Zn)Sn ₃ after air storage at RT	45.0	7.2	1.6	17.5	28.7
(Ce, Zn)Sn ₃ after air storage at 150 °C	40.0	5.5	1.6	19.3	33.6

Table 4 Chemical compositions of the various phases in the Sn-8Zn-1Bi-0.5Ce solder

	Sn, at.%	Zn, at.%	Bi, at.%	Ce, at.%	O, at.%
Solder matrix	83.2	3.7	0.9	0.5	11.7
(Ce, Zn)Sn ₃ before air storage	54.9	9.2	0.6	17.0	18.3
(Ce, Zn)Sn ₃ after air storage at RT	53.5	5.0	0.9	17.8	22.8
(Ce, Zn)Sn ₃ after air storage at 150 °C	43.8	6.4	0.4	19.2	30.2

where the $(\text{Ce}, \text{Zn})\text{Sn}_3$ intermetallic compounds were effectively refined and the rapid whisker growth was eliminated (Ref 9). On account of the formation of large $(\text{Ce}, \text{Zn})\text{Sn}_3$ clusters in this Sn-8Zn-3Bi-0.5Ce alloy, tin whiskers can also be observed on the oxidized $(\text{Ce}, \text{Zn})\text{Sn}_3$ intermetallics of this alloy after air storage at room temperature and at 150 °C. Figure 2 shows that all these tin whiskers have a diameter of about 1 μm , independent of the temperature effect, which is inconsistent with the previous study on a Sn-3Ag-0.5Cu-0.5Ce solder (Ref 8). In that case, long fiber-shaped whiskers with a diameter about 0.1 μm became coarse hillocks with a diameter of 5 to 10 μm . Furthermore, Table 2 also shows that accompanying the whisker growth, the oxygen content on the surface of $(\text{Ce}, \text{Zn})\text{Sn}_3$ clusters increased about 2-folds. This increase confirms that the driving force for the whisker growth in this Sn-8Zn-3Bi-0.5Ce alloy resulted from the predominate oxidation of Ce atoms in the

$(\text{Ce}, \text{Zn})\text{Sn}_3$ clusters. These results together imply that the addition of 3 wt.% Bi into the Sn-8Zn-0.5Ce solder to inhibit tin whisker growth on the surface of RE containing solders through alloying with Zn, as reported previously in the Sn-9Zn-0.5Ce and Sn-3Ag-0.5Cu-0.5Ce-0.5Zn alloys, is in vain (Ref 9, 10).

Lowering the Bi content in such a Sn-8Zn-0.5Ce solder to 2 wt.% causes an obvious decrease of the amounts of $(\text{Ce}, \text{Zn})\text{Sn}_3$ intermetallic compounds, as shown in Fig. 1(c). In addition, the sizes of these Ce-containing intermetallics are refined to about 3 μm , which is much smaller than those in the Sn-8Zn-3Bi-0.5Ce alloy. As can be seen from Table 3, the $(\text{Ce}, \text{Zn})\text{Sn}_3$ phase possesses a chemical composition (at.%) of Sn:Zn:Bi:Ce:O = 55.2:7.5:1.7:17.8:17.8, and the solder matrix contains 1.5 at.% Bi and minor Ce. After air storage at room temperature and at 150 °C, the oxygen content on the surface of these RE containing intermetallics increased obviously to

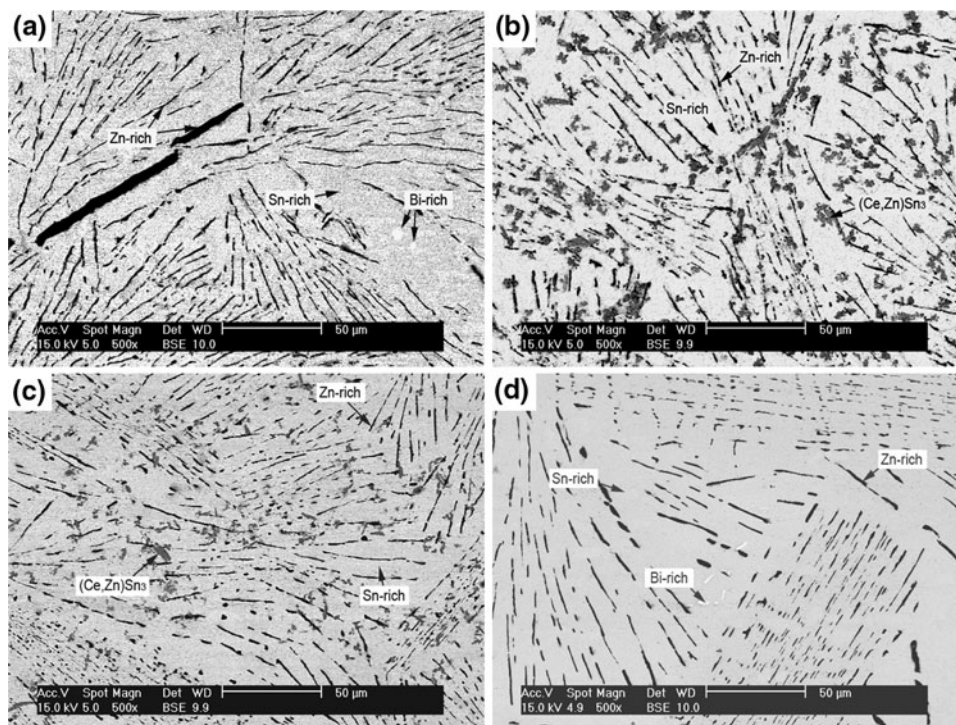


Fig. 1 Microstructure of the as cast solders in this study: (a) Sn-8Zn-3Bi, (b) Sn-8Zn-3Bi-0.5Ce, (c) Sn-8Zn-2Bi-0.5Ce, and (d) Sn-8Zn-1Bi-0.5Ce

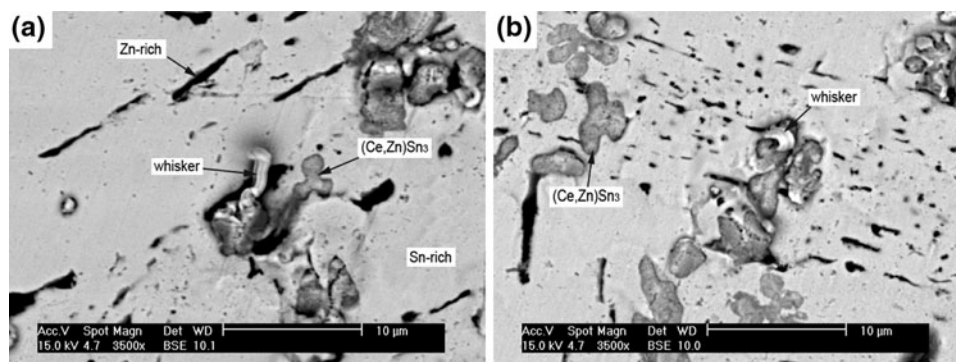


Fig. 2 Tin whiskers formed on the surface of Sn-8Zn-3Bi-0.5Ce solders after air-storage: (a) at room temperature for 336 h and (b) at 150 °C for 144 h

28.7 at.%. Although the outer surface of the $(\text{Ce}, \text{Zn})\text{Sn}_3$ intermetallic clusters in this Sn-8Zn-2Bi-0.5Ce solder have been severely oxidized, tin whiskers are rare, as revealed in Fig. 3. The absence of whisker growth in this case should be correlated to the small size of the $(\text{Ce}, \text{Zn})\text{Sn}_3$ intermetallic clusters in this alloy.

Figure 1(d) reveals that with a further decrease of the Bi content in the Sn-8Zn-0.5Ce alloy to 1 wt.%, the solder matrix is free of $(\text{Ce}, \text{Zn})\text{Sn}_3$ intermetallic clusters. Only in rare cases, as revealed in Fig. 4, can a small amount of fine $(\text{Ce}, \text{Zn})\text{Sn}_3$

particles be found embedded in the thin plates of the Zn-rich phase. Figure 5 further shows that these RE containing intermetallics cannot induce tin whisker growth after exposure at 150 °C in an air furnace for a long period. For the present Sn-8Zn-2Bi-0.5Ce and Sn-8Zn-1Bi-0.5Ce, it is noted that the white particles of Bi phase, which appeared in the solder matrix of Sn-8Zn-3Bi alloy, as shown in Fig. 1(a), were quite scarce. It is suggested that the appearance of Bi-rich particles in Sn-8Zn-3Bi-0.5Ce alloy provides favorable nucleation sites for the formation of $(\text{Ce}, \text{Zn})\text{Sn}_3$ intermetallic clusters in the solder

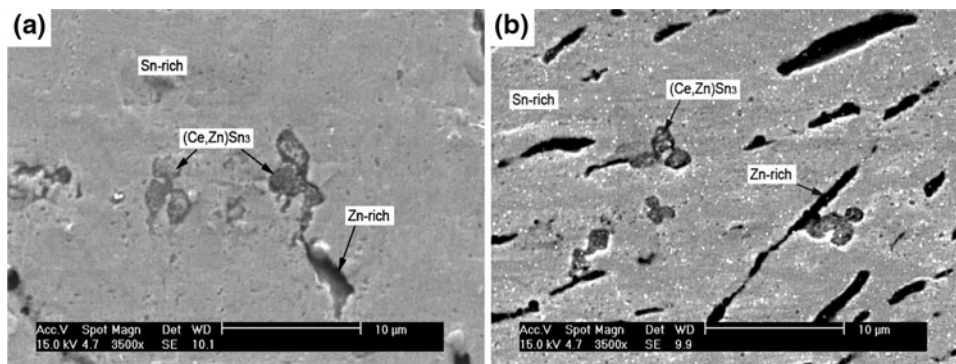


Fig. 3 Morphology of the $(\text{Ce}, \text{Zn})\text{Sn}_3$ intermetallic compounds on the surface of Sn-8Zn-2Bi-0.5Ce solders after air storage: (a) at room temperature for 288 h and (b) at 150 °C for 12 h

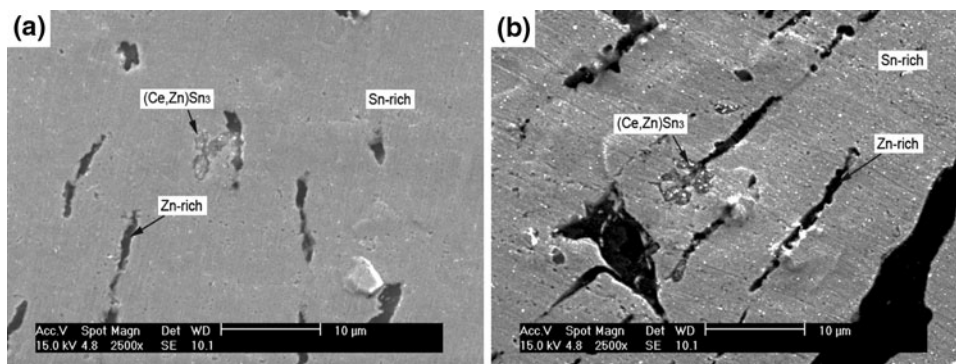


Fig. 4 Morphology of the $(\text{Ce}, \text{Zn})\text{Sn}_3$ intermetallic compounds on the surface of Sn-8Zn-1Bi-0.5Ce solders after air storage: (a) at room temperature for 288 h and (b) at 150 °C for 12 h

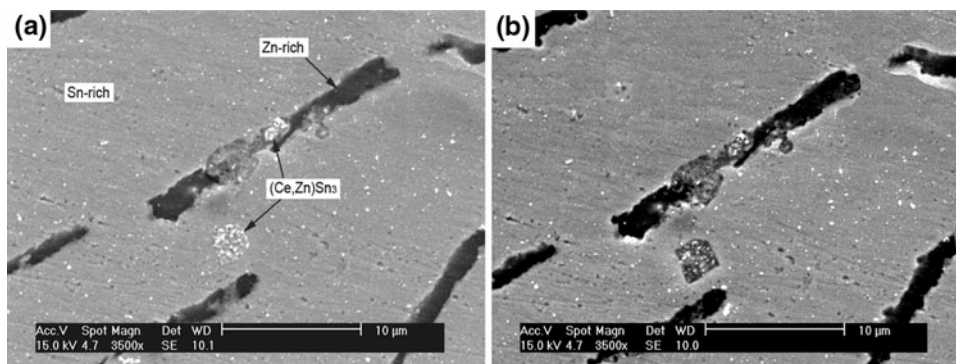


Fig. 5 Morphology of the $(\text{Ce}, \text{Zn})\text{Sn}_3$ intermetallic compounds on the surface of Sn-8Zn-1Bi-0.5Ce solders: (a) before air storage and (b) after air storage at 150 °C for 12 h

matrix, which can much more easily grow to a large size. In contrast, the (Ce, Zn)Sn₃ intermetallics of Sn-8Zn-2Bi-0.5Ce and Sn-8Zn-1Bi-0.5Ce solders tend to nucleate in the plate-shaped Zn-rich phase due to the absence of Bi-particles in the solder matrix. The low thickness of these Zn-rich plates limits the growth of (Ce, Zn)Sn₃ intermetallics.

It has been shown previously that the addition of 0.5 wt.% Ge into a Sn-3Ag-0.5Cu-0.5Ce alloy could effectively diminish the rapid whisker growth of this RE containing solder (Ref 11). The inhibition effect is attributed to the alleviation of oxidation on the CeSn₃ intermetallic clusters as a result of the Ge-alloying. In this study, the alloying with 0.5 wt.% Ge in the Sn-8Zn-3Bi-0.5Ce solder has also been found to be able to extinguish its tin whiskers. Figure 6(a) shows that many cluster-shaped (Ce, Zn)Sn₃ intermetallic phases, with a chemical composition (at.%) of Sn:Zn:Bi:Ce:Ge:O = 66.8:4.1:1.4:

19.8:1.2:6.7, have grown in the solder matrix of Sn-8Zn-3Bi-0.5Ce-0.5Ge alloy. In addition, many cluster-shaped phases with very high concentrations of Ge can externally be found in this Ge-doped alloy. The compositions (at.%) of these Ge-rich clusters, as listed in Table 5, are Sn:Zn:Bi:Ce:Ge:O = 22.1:4.2:0.9:0.8:69.2:2.8. After air-exposure at room temperature, the oxygen content on the surface of both (Ce, Zn)Sn₃ and Ge-rich clusters increased slightly from 6.7 and 2.8 at.% to 8.8 and 7.2 at.%, respectively, and their metallographic morphologies remained almost unchanged, as shown in Fig. 6(b). Similar phenomena were observed for the specimens air-stored at 150 °C for a long period (Fig. 7). The results indicate that not only the Ge-rich phase but also the (Ce, Zn)Sn₃ intermetallics in the Sn-8Zn-3Bi-0.5Ce-0.5Ge alloy possess excellent oxidation resistance, which leads to an inhibition effect on tin whisker growth, as is evidenced in Fig. 6 and 7.

Table 5 Chemical compositions of the various phases in the Sn-8Zn-3Bi-0.5Ce-0.5Ge solder

	Sn, at.%	Zn, at.%	Bi, at.%	Ce, at.%	O, at.%	Ge, at.%
Solder matrix	87.2	1.8	1.8	0.5	7.7	1.0
(Ce, Zn)Sn ₃ before air storage	66.8	4.1	1.4	19.8	6.7	1.2
Ge-rich phase before air storage	22.1	4.2	0.9	0.8	2.8	69.2
(Ce, Zn)Sn ₃ after air storage at RT	54.6	4.6	1.9	17.5	8.8	12.6
Ge-rich phase after air storage at RT	9.4	5.0	2.3	0.5	7.2	75.6
(Ce, Zn)Sn ₃ after air storage at 150 °C	38.1	24.9	1.8	13.4	12.0	9.8
Ge-rich phase after air storage at 150 °C	12.9	5.2	0.6	0.6	8.1	72.6

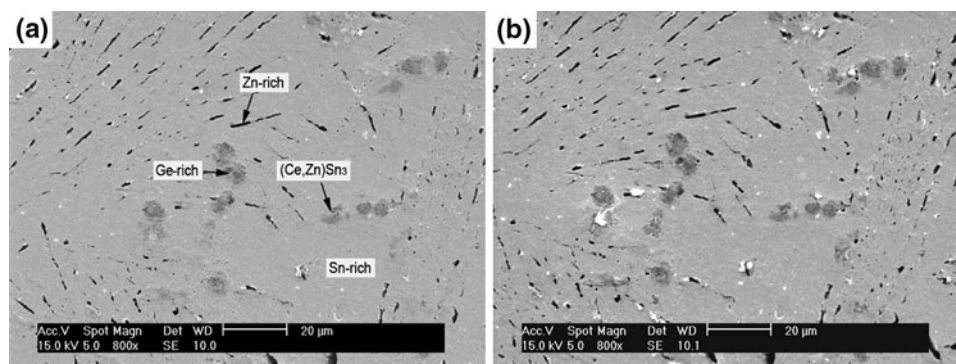


Fig. 6 Morphology of the (Ce, Zn)Sn₃ intermetallic compounds on the surface of Sn-8Zn-3Bi-0.5Ce-0.5Ge solders: (a) before air storage and (b) after air storage at room temperature for 288 h

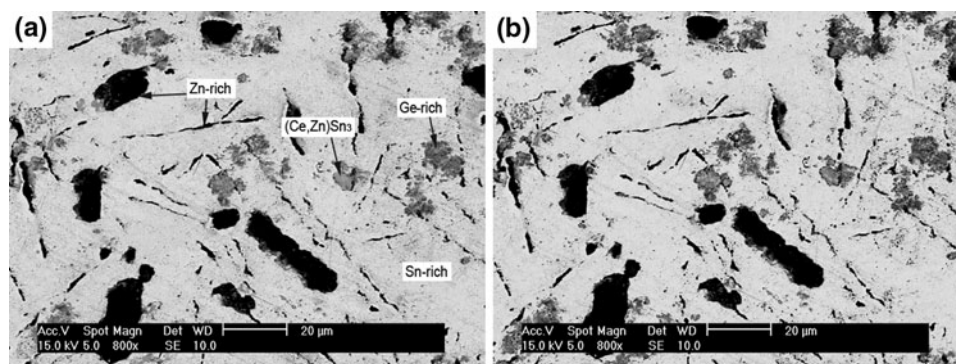


Fig. 7 Morphology of the (Ce, Zn)Sn₃ intermetallic compounds on the surface of Sn-8Zn-3Bi-0.5Ce-0.5Ge solders: (a) before air storage and (b) after air storage at 150 °C for 360 h

4. Conclusions

It has been reported that rapid growth of tin whiskers occurred on the surface of (Ce, Zn)Sn₃ intermetallic clusters in a RE-doped Sn-3Ag-0.5Cu-0.5Ce solder. Further studies showed that the (Ce, Zn)Sn₃ intermetallic phases in Zn-containing Sn-3Ag-0.5Cu-0.5Ce-0.5Zn and Sn-9Zn-0.5Ce were drastically refined, which prevented the appearance of tin whiskers. In this study, an interesting result is that the refining effect of (Ce, Zn)Sn₃ intermetallic phase is nonexistent in a Sn-8Zn-3Bi-0.5Ce alloy, which leads to the phenomenon of rapid whisker growth. The appearance of large (Ce, Zn)Sn₃ clusters might be attributed to the Bi-rich particles in the solder matrix of this alloy, which provide favorable nucleation sites and free growth conditions. The Bi-rich particles disappear with decreases of Bi content in the Sn-8Zn-0.5Ce solders to 1 and 2 wt.%, which result in the recovery of the refining effect of the (Ce, Zn)Sn₃ intermetallic phase and the elimination of tin whiskers. The rapid whisker growth can also be prevented through alloying with 0.5 wt.% Ge in the Sn-8Zn-3Bi-0.5Ce solder due to the inhibition effect of Ge addition on the oxidation of (Ce, Zn)Sn₃ intermetallic clusters.

Acknowledgments

This work was sponsored by the National Science Council, Taiwan, under Grant No. NSC-96-2221-E002-150-MY3. The support from National Taiwan University and Industrial Technology Research Institute, Taiwan, is also greatly appreciated.

References

1. X. Ma, Y.F. Qian, and J. Yoshida, Effect of La on the Cu–Sn Intermetallic Compound (IMC) Growth and Solder Joint Reliability, *J. Alloy. Compd.*, 2002, **334**(1–2), p 224–227
2. C.M.L. Wu, D.Q. Yu, C.M.T. Law, and L. Wang, Improvements of Microstructure, Wettability, Tensile and Creep Strength of Sn–Ag Alloy by Doping with Rare-Earth Elements, *J. Mater. Res.*, 2002, **17**(12), p 3146–3154
3. C.M.L. Wu, D.Q. Yu, C.M.T. Law, and L. Wang, Microstructure and Mechanical Properties of New Lead-Free Sn–Cu–RE Solder Alloys, *J. Electron. Mater.*, 2002, **31**(9), p 928–932
4. Z.G. Chen, Y.W. Shi, Z.D. Xia, and Y.F. Yan, Study on the Microstructure of a Novel Lead-Free Solder Alloy SnAgCu–RE and its Soldered Joints, *J. Electron. Mater.*, 2002, **31**(10), p 1122–1128
5. M.A. Dudek, R.S. Sidhu, N. Chawla, and M. Renavikar, Microstructure and Mechanical Behavior of Novel Rare Earth-Containing Pb-Free Solders, *J. Electron. Mater.*, 2006, **35**(12), p 2088–2097
6. C.M.L. Wu, D.Q. Yu, C.M.T. Law, and L. Wang, The Properties of Sn–9Zn Lead-Free Solder Alloys Doped with Trace Rare Earth Elements, *J. Electron. Mater.*, 2002, **31**(9), p 921–927
7. T.H. Chuang and S.F. Yen, Abnormal Growth of Tin Whiskers in a Sn3Ag0.5Cu0.5Ce Solder BGA Package, *J. Electron. Mater.*, 2006, **35**(8), p 1621–1627
8. T.H. Chuang, Temperature Effects on the Whiskers in Rare-Earth Doped Sn–3Ag–0.5Cu–0.5Ce Solder Joints, *Metall. Mater. Trans. A*, 2007, **38**(5), p 1048–1055
9. T.H. Chuang and H.J. Lin, Size Effect of Rare-Earth Intermetallics in Sn–9Zn–0.5Ce and Sn–3Ag–0.5Cu–0.5Ce Solders of the Growth of Tin Whiskers, *Metall. Mater. Trans. A*, 2008, **39**(12), p 2862–2866
10. T.H. Chuang and H.J. Lin, Inhibition of Whisker Growth on the Surface of Sn–3Ag–0.5Cu–0.5Ce Solder Alloyed with Zn, *J. Electron. Mater.*, 2009, **38**(3), p 420–424
11. T.H. Chuang and C.C. Chi, Effect of Adding Ge on Rapid Whisker Growth of Sn–3Ag–0.5Cu–0.5Ce Alloy, *J. Alloy. Compd.*, 2009, **480**(8), p 974–980